# Using a centrifuge-based method to identify novel root traits that affect root-substrate adhesion in *Arabidopsis thaliana*

Bethany M Eldridge[1,*], Emily R Larson[1,*], Laura Weldon[1,3], Kevin M Smyth[1], Annabelle N Sellin[1], Isaac V Chenchiah[2], Tanniemola B Liverpool[2] and Claire S Grierson[1,#]

[1]School of Biological Sciences, University of Bristol, Bristol Life Sciences Building, 24 Tyndall Avenue, Bristol, BS8 1TQ, UK

[2]School of Mathematics, University of Bristol, Fry Building, Woodland Road, Bristol BS8 1UG, UK

[3]Wildfowl and Wetlands Trust (WWT), Slimbridge, Gloucester, GL2 7BT, UK

[*]Authors contributed equally to this work.

#Corresponding author

Author for correspondence:

*Claire Grierson*

*Tel:* +44 117 39 41185

*Email:* lacsg@bristol.ac.uk

**ORCID:**

BME: ORCID: 0000-0002-6598-3701

ERL: ORCID: 0000-0002-5498-8152

LW: ORCID: 0000-0002-0761-4414

KMS: ORCID: 0000-0003-0105-8557

IVC: ORCID: 0000-0002-8618-620X

TBL: ORCID: 0000-0003-4376-5604

CSG: ORCID: 0000-0002-4000-0975

## Summary (162)

- The physical presence of roots and the compounds they release affect the cohesion between roots and their environment. However, the plant traits that are most important for these interactions are unknown and most methods that quantify the contributions of these traits are time-intensive and require specialist equipment and complex substrates.
- We used an inexpensive, high-throughput phenotyping assay to test its sensitivity and versatility for discovering root traits and novel genes important for root-substrate adhesion. This assay measures the centrifugal force required to detach *Arabidopsis thaliana* seedlings from an agar medium.
- Using this method, we identified root hair shapes, vesicle trafficking pathways and root exudate composition that are important for root-substrate adhesion. We used the assay to conduct a genetic screen and discovered a previously uncharacterised ABC transporter. This demonstrates how this assay can be used to identify novel genes that affect root-substrate interactions.
- This assay is a powerful tool for identifying and quantifying genetic contributions to cohesion between roots and their environment.

## Keywords

Arabidopsis, Centrifuge assay, Forward genetics, Root exudates, Root hairs, Root-soil adhesion, Survival analysis, Vesicle trafficking

## Introduction (593)

Plants secrete compounds that help them adapt to their environment, sense and interact with other organisms, and improve water and nutrient uptake (Bailey et al., 2002; Datta et al., 2011; Haling et al., 2013). These compounds, termed exudates, can vary in composition based on plant species, developmental stage, or environment (Naveed et al., 2017). Recent studies have shown that some compounds have bioadhesive properties that stick plants and soils together and aggregate soil particles, modifying the microenvironment around plant roots (Galloway et al., 2018).

Understanding how plant biology and physiology contribute to plant-soil interactions can be confounded by multiple factors: other organisms living in the soil also secrete organic metabolites that can contribute to soil cohesion, soil composition might affect plant exudate

composition and vice versa. Also, plant root morphology including root architecture and root hairs can alter root-soil interactions (Bailey et al., 2002; Burylo et al.; De Baets et al., 2007; Ghestem et al., 2014; Stokes et al., 2009). This complexity has made it difficult to characterise the relevant plant physiology.

Increasing centrifugal force has been used to measure the capacity of different tropical arboreal ant species to adhere to a smooth Perspex surface when spun at increasing speed in a centrifuge (Federle et al., 2000). We developed a high-throughput assay that identifies and quantifies the contribution of root hair cells to root-substrate cohesion in a less variable environment than the natural rhizosphere (De Baets et al., 2020). The assay uses a centrifuge to apply force to *Arabidopsis thaliana* seedlings grown on the surface of a sterile medium and measures the force required to detach seedlings from that surface. The adherence of candidate lines to the gel at increasing centrifugal force is then compared to a wild type control line. Applying a Cox proportional hazards regression (Prentice and Kalbfleisch, 2003) to the results from centrifuging seedlings allows the adherence of candidate Arabidopsis lines relative to wild-type plants at increasing centrifugal force to be quantified.

While the centrifuge assay was initially developed as one component of a report on how the absence or presence of root hairs affects root-substrate adhesion (De Baets et al., 2020), we wanted to optimize the capability of the assay to evaluate other traits and provide a highly quantifiable and affordable way to screen large populations of seedlings for the identification of new genetic factors important for plant-substrate interactions. To assess this extended use of the assay, we asked (1) if the assay could detect effects of root hair shape on adhesion; (2) if trafficking functions that affect adhesion could be identified in mutants with altered vesicle trafficking but no known root hair morphological defects; (3) if effects of exudate composition could be detected in mutants with altered exudate composition but no known root hair morphological defects; and (4) if the assay could isolate lines from a mutant population in a forward genetic screen to identify novel genes that affect root-substrate adhesion.

Here, we show that this centrifugation method can be used to investigate how root hair morphology contributes to substrate adhesion and screen for biological components that do not present a visible phenotype. Using the genetic and molecular tools available in Arabidopsis and working in a sterile environment allows hypotheses about plant adhesive factors to be tested. While plant-soil cohesion is a complex and dynamic interaction, our assay provides a way to probe root cellular functions that might be masked by confounding

variables in a soil-based study system. Results from this assay provide a platform for more comprehensive studies of plant morphology and physiology that promote root-substrate cohesion.

## Materials and Methods (1380)

### Plant material and growth conditions

Candidate lines of the Columbia-0 (Col-0) ecotype of *Arabidopsis thaliana* single-gene mutants were obtained from the Nottingham Arabidopsis Stock Centre (NASC; Nottingham, UK) or were stocks maintained in the lab (Table 1). Wild-type plants for all experiments were also the Col-0 ecotype. Homozygous lines of *csld3, cow1-3, lrx1-4, rol1-2, gdi1-2, chc1-2, chc2-3, syp121, syp122, jin1-9, pft1-3* and *pdr2* were used in all experiments. Homozygosity of the *abcg43* mutant alleles was confirmed by genomic PCR analysis.

For all experiments, seeds were surface sterilised for 15 min in a solution containing 20% bleach and sterile water, followed by five washes in sterile water. All sterilised seeds were stratified in the dark at 4°C for 24-48 h in Eppendorf microtubes containing sterile water. All plants were reared in a growth room at 21-22°C with a continuous photoperiod (light intensity = 120-145 μmol $m^{-2}$ $s^{-1}$) at 60% humidity.

Sterilized seeds were sown onto 90-mm Petri plates (Thermo Scientific RC2260). containing 30 ml sterile gel medium and sealed with Parafilm (Bemis, NA). The gel consisted of half strength Murashige and Skoog basal medium (Sigma M5519) with 1% [w/v] sucrose pH adjusted to 5.7, solidified with 1% [w/v] agar (Sigma A1296). Seed-sown plates were placed upright at ~80° from the horizontal (lid side down) to encourage vertical growth along the gel surface. Plants for genomic DNA extractions were grown in compost (three parts Levington F3 compost and one-part J Arthur Bowers horticultural silver sand).

### Centrifuge assay set-up

To measure the adhesion of Arabidopsis seedling roots using a centrifuge, seedling roots must not penetrate the gel or each other, as both events could affect root-gel adhesion by interfering with seedling detachment during centrifugation. Therefore, only ten seeds were sown 1 cm apart on a 90 mm Petri plate in two parallel rows**.** The plates were then orientated vertically at approximately 80° from horizontal and grown for 5-6 days in a growth chamber (Fig. S1a). Individual plates and seedlings were visually evaluated to ensure that plants were at the same developmental stage and of similar size. Any seedlings that were touching each other, had grown into the gel, or not uniform in size were omitted from the assay. The

seedlings were then numbered so that plate positional effects could be included as a potential covariate in the final analysis (Fig. S1b). Plates were inverted and placed into a swing-out bucket centrifuge (Beckman Allegra X-30R Centrifuge) that held four plates at a time and subjected to increments of increasing centrifugal force at 720, 1018, 1247, 1440 and 1611 RPM for one minute each (Fig. S1b). The proportion of seedlings that detached from the gel surface was recorded between each centrifugal speed; a detachment event was recorded when a seedling had partially or fully peeled away from the gel (Fig. S1b). If the gel shattered during the assay, seedlings that had not detached from the gel were not recorded and seedlings that remained adhered to the gel after the maximum centrifugal speed were censored in our analyses.

**Calculating seedling detachment force**

To calculate the centrifugal force acting on a seedling, the aerial tissue mass for each seedling was measured using an analytical balance (Microbalance ME5; Sartorius; Fig. S1c). The aerial tissue weight of each seedling was measured because a plant with heavier aerial tissue experiences more force than a lighter one subjected to the same centrifugal speed. Centrifugal force, Fc (mN) acting on a seedling was calculated as previously reported in De Baets et al. (2020). Aerial tissue weight (kg), the angular velocity ($\omega$) and the distance between the seedling and the axis of rotation on the centrifuge (radius = 0.07m) were used to give the following equation:

$$Fc = mass \times radius \times \omega^2 \qquad \text{(Equation 1)}$$

**Identification of *abcg43-1* mutant T-DNA insert**

Genomic DNA was extracted from a pool of vegetative tissue taken from ten three-week old plants using an adapted protocol (Healey et al., 2014) for Illumina Next-Generation two x paired-end sequencing conducted at the Bristol Genomics Facility. The Illumina TruSeq Nano LT gDNA kit (Illumina Inc) was used to generate a genomic DNA sequencing library following the manufacturer's protocol. The final library was diluted to a loading concentration of 1.4 pM for cluster generation and 2 x 150 bp paired-end sequencing on the Illumina NextSeq500 system (Illumina Inc) alongside a 5% PhiX spike-in control library. Read summary statistics were generated using the RTA 2.4.6 Primary Analysis Software (Illumina Inc). The read summaries were analysed in the Sequencing Analysis Viewer (Illumina Inc). Filtered paired reads were subject to paired-end alignment using the Bowtie2

2.3.4.2 aligner (Langmead and Salzberg, 2012). A bespoke reference genome was produced that combined the TAIR10 Arabidopsis genome (Lamesch et al., 2012) and the pROK2 vector sequence (Baulcombe et al., 1986). Alignments were viewed in the Integrative Genomics Viewer IGV 2.3 (Robinson et al., 2011).

For Sanger sequencing, DNA was extracted from a pool of vegetative tissue taken from two-week-old plants using a modified Edwards prep (Edwards et al., 1991). High fidelity PCR was conducted on the *abcg43-1* line using the Q5 High-Fidelity 2X Master Mix (NEB). PCR products were purified and extracted from a 1% agarose gel using the QIAquick Gel Extraction Kit (QIAGEN), following the manufacturer's instructions. Purified PCR product plus the *abcg43-1* forward, reverse or border genotyping primer (Table S1) was used for Sanger sequencing (using the Mix2Seq overnight sequencing kit, Eurofins Genomics). Chromatograms and FASTA files were obtained from Eurofin Genomics and following manual low-quality end trimming, the final sequences were aligned to the pROK2 vector sequence and *ABCG43* gene sequence using the MUSCLE alignment tool (Edgar, 2004).

**Genotyping**

To genotype the *abcg43* mutant alleles, genomic DNA was extracted from the vegetative tissue of two-week-old plants using a modified Edwards prep (Edwards et al., 1991). T-DNA border and gene-specific primers were used in PCR analyses to confirm the genotype (Table S1).

**Morphological root trait analyses**

Five-day-old Arabidopsis seedlings were imaged with a Leica MZ FLIII microscope (Leica) with dark-field lighting. Root hair length and density were measured using microscope images of five-day-old Arabidopsis seedlings and Fiji version 1.0 (Schindelin et al., 2012), using the Bio-Formats Importer plugin to load images into Fiji. At least two experimental repeats were conducted; in each experiment we imaged eight to ten individual plants from each line and measured at least 30 root hairs per plant.

**Statistical analyses**

All statistical analyses were conducted using RStudio, version 1.1453 (R Core Team, 2014) and all graphs were generated using the R package ggplot2 (Wickham, 2016).

A Cox proportional hazards (PH) regression model was used to statistically test for differences between the detachment of experimental seedlings relative to the wild-type

control (Col-0) at increasing force. Cox PH regression models were conducted using the coxph function within the survival package in R and in all cases, the assumption of proportionality was satisfied. Comparisons of different candidate lines relative to the wild type line were analysed *a priori*; therefore, a series of contrasts were set up using the R function contr.treatment rather than using post-hoc testing methods. Seedling position and individual plate number were incorporated as covariates to account for any heterogeneity; when these covariates had no significant effect, they were removed from the model. We censored seedlings that remained attached to the gel after the maximum centrifugal speed because we did not determine the speed these seedlings would have detached from the gel. For each Cox PH regression model run, we report the P value of the Wald Statistic (*z*-score) and the hazard ratio with the upper and lower bound confidence intervals. An alpha level of 0.01 was used. The root-gel detachment of at least 70 plants from each line was assessed within a single experiment.

Univariate analyses were conducted using the lm function in R to test for differences in the mean root hair density or mean root hair length (of eight to ten individual plants from each line) between candidate lines relative to wild type. In all cases, the assumptions of normality and homoscedasticity were satisfied. Because comparisons of different mutant lines relative to the wild type line were *a priori*, a series of contrasts were conducted using the contr.treatment function in R. To prevent type I errors from multiple testing, we applied the Bonferroni method and adjusted the alpha level to 0.025 (0.05/2).

## Results **(1795)**

### Using the Cox survival regression model to quantify root-substrate adhesion

To compare the root-gel adhesion properties of candidate lines relative to wild type we conducted a semi-parametric Cox proportional hazards (PH) regression. We chose this over other types of survival analyses to statistically evaluate the differences in detachment of Arabidopsis seedlings at increasing force because Cox PH regression models are multivariate and can test whether covariates affect the occurrence of an event (i.e. gel detachment) as well as manage censored data (Bradburn et al., 2003; Cox, 1972; Devarajan and Ebrahimi, 2009). Unlike univariate tests commonly used in survival analysis such as the Logrank test, Cox PH regression models also provide an estimate of the difference in effect size between two groups by calculating a hazard ratio, which is an exponential coefficient that gives the instantaneous risk of an event (Cox and Oakes, 1984; Spruance et al., 2004). This is

advantageous because we used hazard ratios as a strength measure of root-gel adhesion by comparing the seedling detachment risk of candidate lines relative to wild type.

We report the P-value calculated from the Wald statistic (*z*-score) and the hazard ratio with upper and lower bound confidence intervals. Wild type was used as the baseline group for all models, with a hazard ratio of one. Therefore, a candidate line with a higher risk of detachment from the gel than wild type will have a hazard ratio above one, while lines with a lower risk of detachment than wild type will have a hazard ratio below one. Because roots are developmentally plastic and sensitive to environmental heterogeneity (Bliss et al., 2002; Gao et al., 2004; Šmilauerová, 2001), we assessed the root-gel detachment of at least 70 seedlings from each line in a single experiment.

**Root hair morphological effects on root-substrate adhesion**

We screened mutant lines with known root hair morphology defects to ask if the centrifuge assay could determine if root hair shape affects root-substrate adhesion. The mostly bald mutant *csld3*, which encodes the CESA-like 3D protein (Favery et al., 2001; Yang et al., 2020) was included as a root hairless example. For lines that produce short or malformed root hairs, we included the *gdi1-2* Rho GTPase GDP dissociation inhibitor mutant, *rol1-2* rhamnose biosynthesis 1 mutant allele, *can of worms 1* (*cow1-3*) phosphatidylinositol transferase protein mutant, and *lrx1-4* leucine rich extensin 1 mutant (Baumberger et al., 2001; Böhme et al., 2004; Carol et al., 2005; Diet et al., 2006; Grierson et al., 1997). The *rol1-2* and *gdi1-2* mutants have short root hairs and the root hairs on *gdi1-2* plants can also branch (Parker et al., 2000; Ringli et al., 2008). *cow1-3* plants have short, wide root hairs that can branch, whilst *lrx1-4* plants can develop root hairs that abort, swell, branch, or collapse in a growth condition-dependent manner (Baumberger et al., 2001; Grierson et al., 1997; Parker et al., 2000). Under our growth conditions, we confirmed the reported phenotypes for each mutant line (Fig. 1a).

Consistent with previous results (De Baets et al., 2020), bald (*csld3*) seedlings detached at lower centrifugal forces relative to wild-type seedlings, with 4.6 times the risk of detachment compared to wild-type plants ($z$ = 8.644, P<0.001, HR = 4.636, 95% CI = 3.274 – 6.564; Fig. 2b). Mutants with deformed root hair phenotypes including *gdi1-2, rol1-2, cow1-3* and *lrx1-4* had risks of detachment that were 2.5, 4, 3.8 and 3.9 times that of wild-type plants, respectively (*gdi1-2* – $z$ = 5.199, P<0.001, HR = 2.459, 95% CI = 1.752 – 3.452; *rol1-2* – $z$ = 7.927, P<0.001, HR = 4.036, 95% CI = 2.858 – 5.698; *cow1-3* – $z$ = 7.350, P<0.001, HR = 3.790, 95% CI = 2.657 – 5.407; *lrx1-4* – $z$ = 8.049, P<0.001, HR = 3.926, 95% CI =

2.814 – 5.478; Fig. 2b-d). These results indicate that the centrifuge assay can quantify effects of root hair shape on root-substrate cohesion. Many of the root hair mutants tested are associated with changes in root hair cell wall composition, suggesting that alterations in secreted compounds could affect root-substrate interactions in addition to any physical or surface area-related factors that are specific to root hairs.

**Vesicle trafficking mutations affect root-substrate adhesion**

We hypothesized that Arabidopsis mutants with defective trafficking pathways might alter cell wall and apoplast characteristics that contribute to root-substrate interactions and adhesion. We chose the secretory Soluble NSF (N-ethylmaleimide sensitive fusion protein) Attachment proteins (SNAP) REceptor (SNARE) mutants *syp121* and *syp122-1*, and the endocytic mutants, *chc1-2* and *chc2-3* as candidates for our assay. SYP121 is the primary secretory SNARE found on the plasma membrane (Assaad et al., 2004; Geelen et al., 2002) and has characterized aboveground phenotypes, including small rosettes and stomatal mobility defects (Eisenach et al., 2012; Larson et al., 2017); however, the mutant does not have a reported root hair phenotype. Although the related SNARE SYP122 is thought to share partial functionality with SYP121, the *syp122-1* mutant does not share these phenotypes with *syp121* and a recent proteomic analysis reported differences in their vesicle cargoes, which could contribute to their functional independence (Waghmare et al., 2018). The *chc1-2* and *chc2-3* mutants are defective in the heavy chain subunits of the clathrin coat complex, which is required for vesicle traffic at the plasma membrane (Kitakura et al., 2011). Endo- and exocytic rates are impaired in both mutants (Larson et al., 2017), but no root hair phenotypes have been reported. For the centrifuge assay, it was important to select mutants that do not have root hair phenotypes given the effect root hair morphology has on root-gel adhesion. Therefore, we evaluated the root hairs of these trafficking mutants and found that the root hairs of these lines did not significantly differ from wild-type plants (Fig. 2a).

Overall, the risk of detachment for *syp121, syp122-1, chc1-2* and *chc2-3* plants was 3.6, 3.3, 4.5 and 3.9 times that of wild type, respectively (*syp121* – $z$ = 7.702, P<0.001, HR = 3.593, 95% CI = 2.595 – 4975; *syp122-1* – $z$ = 7.199, P<0.001, HR = 3.270, 95% CI = 2.369 – 4.515; *chc1-2* – $z$ = 8.238, P<0.001, HR = 4.482, 95% CI = 3.137 – 6.405; *chc2-3* – $z$ = 7.653, P<0.001, HR = 3.941, 95% CI = 2.774 – 5.599; Fig. 2b, c). Given that all the mutants detached from the gel at lower centrifugal forces than wild-type seedlings, these results indicate that the corresponding genes contribute to root-substrate adhesion and that the

centrifuge assay can be used to probe for intracellular molecular machinery that affect root-substrate interactions.

**Exudate composition changes root detachment rates**

Over 20% of plant assimilated carbon is released as root exudates (Huang et al., 2016) that modify the external environment in response to abiotic and biotic stimuli and contribute to soil adhesion (Akhtar et al., 2018; Galloway et al., 2018). Root epidermal and hair cells secrete compounds that contribute to root exudate profiles that can be plant species specific (Naveed et al., 2017). Because mutants in both root hair development and vesicle trafficking pathways showed root-substrate adhesion phenotypes (Figs. 1 and 2), we asked if the centrifuge assay could identify effects of exudate composition on root-substrate adhesion. We selected Arabidopsis mutants reported to have altered exudate composition compared to wild type, including *pft1-3*, *jin1-9*, and *pdr2* (Badri et al., 2009; Berger et al., 1996; Carvalhais et al., 2015; Kidd et al., 2009). *PFT1* (*MED25*) encodes the MEDIATOR25 subunit of the Mediator nuclear protein, and *JIN1* (*MYC2*) encodes a basic helix-loop-helix leucine zipper transcription factor; both proteins are involved in the jasmonate signalling pathway (Kidd et al., 2009; Lorenzo et al., 2004). *pft1-3* and *jin1-9* mutants are reported to have altered root exudate composition, including lower amounts of the amino acids asparagine, ornithine and tryptophan than wild-type plants (Carvalhais et al., 2015). *PDR2* (*ABCG30*) encodes a pleiotropic drug resistance (PDR) full-length ABC transporter that is involved in ABA transport and the exudation of secondary metabolites (Badri et al., 2008; Kang et al., 2015). We did not observe root hair growth phenotypes in these mutant lines compared to wild type (Fig. 3a).

We found that compared to wild-type seedlings, *pdr2* seedlings resisted detachment, with 0.38 times the risk of detaching from the gel ($z$ = -5.765, P<0.001, HR = 0.379, 95% CI = 0.273 – 0.528; Fig. 3b). Conversely, *pft1-3* seedlings had an increased risk of detachment 1.7 times that of wild-type plants ($z$ = 3.315, P<0.001, HR = 1.698, 95% CI = 1.242 – 2.323), and there was no difference in gel adhesion between *jin1-9* and wild-type plants ($z$ = 0.737, P>0.05, HR = 1.124, 95% CI = 0.824 – 1.537; Fig. 3b). These results show that exudate composition can alter root-substrate interactions, although this may not be the case for all exudate compositional changes, or identification of the effects of the exudate composition of the *jin1-9* mutant lay outside the sensitivity range of the assay. Since these mutant lines did not have root hair phenotypes, our results suggest that changes in exudate composition alter

root adhesive properties without affecting plant root hair morphology, further indicating the power of the centrifuge assay as a potential mutant screening method.

**Centrifuge assay as a method for forward genetic screening**

Having demonstrated that our centrifugation technique can be used to identify different types of traits that affect root-substrate adhesion, we conducted a forward genetic screen to identify novel genes involved in root-substrate adhesion. To conduct this screen, the root-gel adhesion properties of individual plants from a pooled SALK T-DNA insertion mutant collection were analysed (Alonso et al., 2003). Individual plants with significantly increased or decreased root-gel adhesion relative to wild-type plants were recovered from the screen and self-fertilized to obtain progeny and identify the mutations. We identified a line with significantly enhanced root-gel adhesion and conducted genomic Next-Generation sequencing followed by Sanger sequencing of T-DNA flanking PCR products to confirm a T-DNA insertion in the ABC transporter gene, *ABCG43,* whose function is unknown. We named this T-DNA insertion line *abcg43*-1 and identified additional mutant alleles, *abcg43-2* (SALK_201207c) and *abcg43-3* (SALKseq_30713) (Fig. 4a).

We analysed the root-gel adhesion of homozygous insertional mutant alleles for *ABCG43* and found *abcg43-1, abcg43*-2 *and abcg43*-3 plants resisted detachment from the gel, with detachment risks 0.25, 0.35 and 0.2 times that of wild-type plants, respectively (*abcg43-1* – $z$ = -7.823, P<0.001, HR = 0.245, 95% CI = 0.172 – 0.348; *abcg43-2* – $z$ = -6.049, P<0.001, HR = 0.355, 95% CI = 0.253 – 0.496; *abcg43-3* – $z$ = -7.179, P<0.001, HR = 0.203 – 0.403; Fig. 4b, c). Collectively, these results suggest that disruption of *ABCG43* expression and protein function affects root-gel adhesion. These results also illustrate the use of the centrifuge assay as a powerful screening method for identifying novel genes involved in root-substrate adhesion, as well as a tool for evaluating the effects of known gene function on root-substrate interactions. Experiments are now being conducted to identify mutant trait(s) in these lines and understand how *ABCG43* affects root-substrate adhesion.

## Discussion **(837)**

To date, most published methods that quantify the contribution of particular traits to plant-soil interactions are time-intensive and expensive (Bailey et al., 2002; De Baets and Poesen, 2010; De Baets et al., 2020; Lin and Ying, 1994; Toukura et al., 2006). In contrast,

our assay can produce data within a week, is available to any laboratory with access to a bench top centrifuge and does not require speciality consumables. This method is a high-throughput and quantitative way to test the effects of root morphology and cell function on root-substrate adhesion and to screen for new biological and molecular factors that can alter plant-substrate interactions. Using a defined model system like Arabidopsis and sterile medium conditions permits plant-specific characteristics to be identified that can then be probed in other substrate- or soil-based conditions.

Survival analyses are not often utilised by plant biologists because measurements are static or endpoints, like root length, flowering time, or fresh/dry weight and therefore, do not require a dynamic analysis of individual datapoints over a continuous spectrum of time or force. However, survival analysis is used across other scientific fields to study the timing of an event, such as the time for an animal to learn a behaviour, for an individual to recover or die from a disease, or an electrical failure to occur (Allison, 2010; Lin and Ying, 1994; Miller, 1998). Here, we use survival analysis to study root-substrate interactions, where seedling detachment is the event that occurs over increasing forces.

**Using the centrifuge assay to investigate the role of root hairs in root-substrate interactions**

Results presented in this paper show that the centrifuge assay can quantify effects of root hair morphology on plant-substrate adhesion. By using well-characterized Arabidopsis root hair mutants, we show this assay can evaluate the adhesive properties of mutants with a wide variety of root hair phenotypes. Previous work has shown that the presence of root hairs can significantly enhance root-substrate adhesion compared to the absence of root hairs (Choi and Cho, 2019; De Baets et al., 2020; Haling et al., 2013). Indeed, our centrifuge assay has previously been used to quantify the forces required to detach seedlings with and without root hairs (De Baets et al., 2020); however, the sensitivity of the assay for comparing how root hair morphology and function affects root-substrate adhesion was not evaluated. We now show that this assay can distinguish the adherence strength of seedlings with altered root hair shapes and sizes (Fig. 1) and quantify the contribution these morphological traits make to plant-substrate interactions. Some mutants with defective root hairs have mutations in cell wall biosynthesis and modification proteins, so it is possible that altered root-substrate interfaces compromise adhesion in these mutants, not just root hair shape. Using our method to rapidly phenotype mutants with root hair growth defects could direct additional experiments to characterize biochemical and morphological properties of genes of interest.

Indeed, current evidence for the importance of root hairs for the deposition of complex polysaccharides with soil-binding properties (Galloway et al., 2020) supports the need for assays such as this one to expedite our ability to identify genes and mechanisms that could improve soil-remediation, top soil maintenance, and erosion tolerance of at-risk land.

**Identifying new genes involved in root-substrate adhesion**

Mutations in cellular functions that do not alter root hair growth but do affect substrate adhesion can also be investigated using this assay. Vesicle trafficking pathways are required for cell wall deposition and maintenance (De Caroli et al., 2011; Larson et al., 2014; Rodriguez-Furlán et al., 2016); therefore, we hypothesized that mutants in trafficking pathways, particularly those at the plasma membrane, could affect root-substrate adhesion. Similarly, the composition and deposition of plant exudates help plants modify and optimize their growth conditions (Carvalhais et al., 2015; Naveed et al., 2017), suggesting that modification to plant exudate composition could affect root-substrate interactions. Consistent with these hypotheses, mutants with vesicle trafficking defects and altered exudate composition have root-substrate adhesion properties that differ from wild type, indicating that this method can identify aspects of plant biology important for root-substrate interactions that do not affect root or root hair morphology (Figs. 2 and 3). Our results further indicate that while root hairs provide significant adhesive and cohesive support both on solid gel and soil media (De Baets et al., 2020), there are additional cellular factors contributing to plant-substrate interactions that are not directly observable without the use of expensive antibodies, development of time-intensive transgenic lines, and microscopy equipment. Our centrifuge assay provides an affordable and quick alternative to these current methodologies.

We used this assay as a screen to identify new genes affecting plant-substrate interactions. As an example, we report the identification in a forward genetics screen of a mutant population in which *abcg43* mutant seedlings were more adhesive to gel than wild type (Fig. 4). The function of ABCG43 in Arabidopsis is uncharacterised and therefore, this assay is a promising tool for identifying novel candidate genes that have no previously known association with root morphological defects, adhesion or exudate composition for future study.

## Conclusion (115)

This assay has applications in plant cell biology and genetics to understand how gene activity, cell function and root structure affect plant-soil adhesion and identify the molecular

pathways involved. Potential applications include measuring variables not tested in this report, such as the effects of environmental conditions on plant-substrate adhesion and how other plant species or ecotypes respond to detachment forces. Given the recent discovery that root hair presence is important for Arabidopsis cohesion between roots and gel, and compost or soil (De Baets *et al.*, 2020), this assay could contribute to plant and soil sciences more broadly through the identification of plant traits that increase root-substrate cohesion and potentially stabilise slopes or reduce soil erosion.

## Supporting Information

**Fig. S1** Centrifuge assay workflow for determining the root-gel adhesion properties of *Arabidopsis thaliana* seedlings

**Table S1** Genotyping primers used in this study for genotyping *Arabidopsis thaliana* mutants

**Table S2** Centrifuge assay troubleshooting


## Acknowledgements **(88)**

This work was supported by a Leverhulme Trust project grant RPG-2013-260 to CSG and TBL and BME was supported by a BBSRC SWBio PhD studentship (grant BB/M009122/1). We are thankful to Don Grierson FRS and Enrico Coen FRS who independently suggested the centrifuge assay concept, Timothy Quine for providing insightful guidance during method development, and Thomas Denbigh for providing essential technical advice. We are grateful to Jill Harrison, Victoria Spencer, Zoe Nemec Venza, Sophie Carpenter and Nicholas H Fair for their helpful comments during revision of the manuscript.


## Author Contributions **(105)**

CSG designed the initial project, conducted proof-of-concept pilot experiments, obtained the funding, and recruited and advise the team. TBL and IC developed the theoretical parametrisation of the centrifugal assay and bounds on the errors from other mechanical forces. BME and ERL planned and conducted all experiments apart from the initial genetic screen, which was carried out by LW and KMS. BME and ERL analysed all of the data presented herein. AS and BME optimised the centrifuge assay data collection and data analysis methods. BME and ERL wrote the initial manuscript. BME, ERL, and CSG edited the manuscript. All authors reviewed and approved the final manuscript.

## References


Akhtar, J., Galloway, A.F., Nikolopoulos, G., Field, K.J., and Knox, P. (2018). A quantitative method for the high throughput screening for the soil adhesion properties of plant and microbial polysaccharides and exudates. Plant Soil *428*, 57–65.

Allison, P.D. (2010). Survival Analysis Using SAS: A Practical Guide, Second Edition (SAS Institute).

Alonso, J.M., Stepanova, A.N., Leisse, T.J., Kim, C.J., Chen, H., Shinn, P., Stevenson, D.K., Zimmerman, J., Barajas, P., Cheuk, R., et al. (2003). Genome-wide insertional mutagenesis of Arabidopsis thaliana. Science *301*, 653–657.

Assaad, F.F., Qiu, J.-L., Youngs, H., Ehrhardt, D., Zimmerli, L., Kalde, M., Wanner, G., Peck, S.C., Edwards, H., Ramonell, K., et al. (2004). The PEN1 Syntaxin Defines a Novel Cellular Compartment upon Fungal Attack and Is Required for the Timely Assembly of Papillae. Mol. Biol. Cell *15*, 5118–5129.

Badri, D.V., Loyola-Vargas, V.M., Broeckling, C.D., De-la-Peña, C., Jasinski, M., Santelia, D., Martinoia, E., Sumner, L.W., Banta, L.M., Stermitz, F., et al. (2008). Altered Profile of Secondary Metabolites in the Root Exudates of Arabidopsis ATP-Binding Cassette Transporter Mutants. Plant Physiology *146*, 762–771.

Badri, D.V., Quintana, N., El Kassis, E.G., Kim, H.K., Choi, Y.H., Sugiyama, A., Verpoorte, R., Martinoia, E., Manter, D.K., and Vivanco, J.M. (2009). An ABC transporter mutation alters root exudation of phytochemicals that provoke an overhaul of natural soil microbiota. Plant Physiol. *151*, 2006–2017.

Bailey, P.H.J., Currey, J.D., and Fitter, A.H. (2002). The role of root system architecture and root hairs in promoting anchorage against uprooting forces in Allium cepa and root mutants of Arabidopsis thaliana. J. Exp. Bot. *53*, 333–340.

Baulcombe, D.C., Saunders, G.R., Bevan, M.W., Mayo, M.A., and Harrison, B.D. (1986). Expression of biologically active viral satellite RNA from the nuclear genome of transformed plants. Nature *321*, 446–449.

Baumberger, N., Ringli, C., and Keller, B. (2001). The chimeric leucine-rich repeat/extensin cell wall protein LRX1 is required for root hair morphogenesis in Arabidopsis thaliana. Genes Dev. *15*, 1128–1139.

Berger, S., Bell, E., and Mullet, J.E. (1996). Two Methyl Jasmonate-Insensitive Mutants Show Altered Expression of AtVsp in Response to Methyl Jasmonate and Wounding. Plant Physiology *111*, 525–531.

Bliss, K.M., Jones, R.H., Mitchell, R.J., and Mou, P.P. (2002). Are competitive interactions influenced by spatial nutrient heterogeneity and root foraging behavior? New Phytologist *154*, 409–417.

Böhme, K., Li, Y., Charlot, F., Grierson, C., Marrocco, K., Okada, K., Laloue, M., and Nogué, F. (2004). The Arabidopsis COW1 gene encodes a phosphatidylinositol transfer protein essential for root hair tip growth. Plant J. *40*, 686–698.

Bradburn, M.J., Clark, T.G., Love, S.B., and Altman, D.G. (2003). Survival analysis part II: multivariate data analysis--an introduction to concepts and methods. Br. J. Cancer *89*, 431–436.

Burylo, M., Rey, F., Mathys, N., and Dutoit, T. Plant root traits affecting the resistance of soils to concentrated flow erosion. Earth Surface Processes and Landforms *37*, 1463–1470.

Carol, R.J., Takeda, S., Linstead, P., Durrant, M.C., Kakesova, H., Derbyshire, P., Drea, S., Zarsky, V., and Dolan, L. (2005). A RhoGDP dissociation inhibitor spatially regulates growth in root hair cells. Nature *438*, 1013–1016.

Carvalhais, L.C., Dennis, P.G., Badri, D.V., Kidd, B.N., Vivanco, J.M., and Schenk, P.M. (2015). Linking Jasmonic Acid Signaling, Root Exudates, and Rhizosphere Microbiomes. Mol. Plant Microbe Interact. *28*, 1049–1058.

Choi, H.-S., and Cho, H.-T. (2019). Root hairs enhance Arabidopsis seedling survival upon soil disruption. Scientific Reports *9*, 11181.

Cox, D.R. (1972). Regression Models and Life-Tables. Journal of the Royal Statistical Society: Series B (Methodological) *34*, 187–202.

Cox, D.R., and Oakes, D. (1984). Analysis of Survival Data (Boca Raton, Florida: Chapman & Hall/CRC Press).

Datta, S., kim, C.M., Pernas, M., Pires, N.D., Proust, H., Tam, T., Vijayakumar, P., and Dolan, L. (2011). Root hairs: development, growth and evolution at the plant-soil interface. Plant and Soil *346*, 1–14.

De Baets, S., and Poesen, J. (2010). Empirical models for predicting the erosion-reducing effects of plant roots during concentrated flow erosion. Geomorphology *118*, 425–432.

De Baets, S., Poesen, J., Knapen, A., and Galindo, P. (2007). Impact of root architecture on the erosion-reducing potential of roots during concentrated flow. Earth Surface Processes and Landforms *32*, 1323–1345.

De Baets, S., Denbigh, T.D., Smyth, K.M., Eldridge, B.M., Weldon, L.M., Higgins, B.W., Matyjaszkiewicz, A.W., Meersmans, J., Larson, E.R., Chenchiah, I.V., et al. (2020). Micro-scale interactions between Arabidopsis root hairs and soil particles influence soil erosion. Nature Comms Biol *3*, 1–11.

De Caroli, M., Lenucci, M.S., Di Sansebastiano, G.-P., Dalessandro, G., De Lorenzo, G., and Piro, G. (2011). Dynamic protein trafficking to the cell wall. Plant Signal Behav *6*, 1012–1015.

Devarajan, K., and Ebrahimi, N. (2009). Testing for Covariate Effect in the Cox Proportional Hazards Regression Model. Commun Stat Theory Methods *38*, 2333–2347.

Diet, A., Link, B., Seifert, G.J., Schellenberg, B., Wagner, U., Pauly, M., Reiter, W.-D., and Ringli, C. (2006). The Arabidopsis root hair cell wall formation mutant lrx1 is suppressed by mutations in the RHM1 gene encoding a UDP-L-rhamnose synthase. Plant Cell *18*, 1630–1641.

Edwards, K., Johnstone, C., and Thompson, C. (1991). A simple and rapid method for the preparation of plant genomic DNA for PCR analysis. Nucleic Acids Res *19*, 1349.

Eisenach, C., Chen, Z.-H., Grefen, C., and Blatt, M.R. (2012). The trafficking protein SYP121 of Arabidopsis connects programmed stomatal closure and $K^+$ channel activity with vegetative growth. Plant J. *69*, 241–251.

Favery, B., Ryan, E., Foreman, J., Linstead, P., Boudonck, K., Steer, M., Shaw, P., and Dolan, L. (2001). KOJAK encodes a cellulose synthase-like protein required for root hair cell morphogenesis in Arabidopsis. Genes Dev. *15*, 79–89.

Federle, W., Rohrseitz, K., and Holldobler, B. (2000). Attachment forces of ants measured with a centrifuge: better 'wax-runners' have a poorer attachment to a smooth surface. Journal of Experimental Biology *203*, 505–512.

Galloway, A.F., Pedersen, M.J., Merry, B., Marcus, S.E., Blacker, J., Benning, L.G., Field, K.J., and Knox, J.P. (2018). Xyloglucan is released by plants and promotes soil particle aggregation. New Phytol. *217*, 1128–1136.

Galloway, A.F., Akhtar, J., Marcus, S.E., Fletcher, N., Field, K., and Knox, P. (2020). Cereal root exudates contain highly structurally complex polysaccharides with soil-binding properties. The Plant Journal.

Gao, D., Knight, M.R., Trewavas, A.J., Sattelmacher, B., and Plieth, C. (2004). Self-reporting Arabidopsis expressing pH and [Ca2+] indicators unveil ion dynamics in the cytoplasm and in the apoplast under abiotic stress. Plant Physiol. *134*, 898–908.

Geelen, D., Leyman, B., Batoko, H., Di Sansebastiano, G.-P., Moore, I., Blatt, M.R., and Di Sansabastiano, G.-P. (2002). The abscisic acid-related SNARE homolog NtSyr1 contributes to secretion and growth: evidence from competition with its cytosolic domain. Plant Cell *14*, 387–406.

Ghestem, M., Cao, K., Ma, W., Rowe, N., Leclerc, R., Gadenne, C., and Stokes, A. (2014). A framework for identifying plant species to be used as "ecological engineers" for fixing soil on unstable slopes. PLoS ONE *9*, e95876.

Grierson, C.S., Roberts, K., Feldmann, K.A., and Dolan, L. (1997). The COW1 locus of arabidopsis acts after RHD2, and in parallel with RHD3 and TIP1, to determine the shape, rate of elongation, and number of root hairs produced from each site of hair formation. Plant Physiol *115*, 981–990.

Haling, R.E., Brown, L.K., Bengough, A.G., Young, I.M., Hallett, P.D., White, P.J., and George, T.S. (2013). Root hairs improve root penetration, root-soil contact, and phosphorus acquisition in soils of different strength. J. Exp. Bot. *64*, 3711–3721.

Healey, A., Furtado, A., Cooper, T., and Henry, R.J. (2014). Protocol: a simple method for extracting next-generation sequencing quality genomic DNA from recalcitrant plant species. Plant Methods *10*, 21.

Huang, Y., Wang, Y., Tan, L., Sun, L., Petrosino, J., Cui, M.-Z., Hao, F., and Zhang, M. (2016). Nanospherical arabinogalactan proteins are a key component of the high-strength adhesive secreted by English ivy. Proc. Natl. Acad. Sci. U.S.A. *113*, E3193-3202.

Kang, J., Yim, S., Choi, H., Kim, A., Lee, K.P., Lopez-Molina, L., Martinoia, E., and Lee, Y. (2015). Abscisic acid transporters cooperate to control seed germination. Nat Commun *6*, 8113.

Kidd, B.N., Edgar, C.I., Kumar, K.K., Aitken, E.A., Schenk, P.M., Manners, J.M., and Kazan, K. (2009). The mediator complex subunit PFT1 is a key regulator of jasmonate-dependent defense in Arabidopsis. Plant Cell *21*, 2237–2252.

Kitakura, S., Vanneste, S., Robert, S., Löfke, C., Teichmann, T., Tanaka, H., and Friml, J. (2011). Clathrin mediates endocytosis and polar distribution of PIN auxin transporters in Arabidopsis. Plant Cell *23*, 1920–1931.

Lamesch, P., Berardini, T.Z., Li, D., Swarbreck, D., Wilks, C., Sasidharan, R., Muller, R., Dreher, K., Alexander, D.L., Garcia-Hernandez, M., et al. (2012). The Arabidopsis Information Resource (TAIR): improved gene annotation and new tools. Nucleic Acids Res. *40*, D1202-1210.

Langmead, B., and Salzberg, S.L. (2012). Fast gapped-read alignment with Bowtie 2. Nat Methods *9*, 357–359.

Larson, E.R., Domozych, D.S., and Tierney, M.L. (2014). SNARE VTI13 plays a unique role in endosomal trafficking pathways associated with the vacuole and is essential for cell wall organization and root hair growth in arabidopsis. Ann. Bot. *114*, 1147–1159.

Larson, E.R., Van Zelm, E., Roux, C., Marion-Poll, A., and Blatt, M.R. (2017). Clathrin Heavy Chain Subunits Coordinate Endo- and Exocytic Traffic and Affect Stomatal Movement. Plant Physiol. *175*, 708–720.

Lin, D.Y., and Ying, Z. (1994). Semiparametric Analysis of the Additive Risk Model. Biometrika *81*, 61–71.

Lorenzo, O., Chico, J.M., Sánchez-Serrano, J.J., and Solano, R. (2004). JASMONATE-INSENSITIVE1 encodes a MYC transcription factor essential to discriminate between different jasmonate-regulated defense responses in Arabidopsis. Plant Cell *16*, 1938–1950.

Miller, R.G. (1998). Survival Analysis (New York: Wiley & Sons).

Naveed, M., Brown, L.K., Raffan, A.C., George, T.S., Bengough, A.G., Roose, T., Sinclair, I., Koebernick, N., Cooper, L., Hackett, C.A., et al. (2017). Plant exudates may stabilize or weaken soil depending on species, origin and time. European Journal of Soil Science *68*, 806–816.

Parker, J.S., Cavell, A.C., Dolan, L., Roberts, K., and Grierson, C.S. (2000). Genetic interactions during root hair morphogenesis in Arabidopsis. Plant Cell *12*, 1961–1974.

Prentice, R.L., and Kalbfleisch, J.D. (2003). Mixed discrete and continuous Cox regression model. Lifetime Data Anal *9*, 195–210.

R Core Team (2014). R: A language and environment for statistical computing (Vienna, Austria: R Foundation for Statistical Computing).

Ringli, C., Bigler, L., Kuhn, B.M., Leiber, R.-M., Diet, A., Santelia, D., Frey, B., Pollmann, S., and Klein, M. (2008). The Modified Flavonol Glycosylation Profile in the Arabidopsis rol1 Mutants Results in Alterations in Plant Growth and Cell Shape Formation. The Plant Cell *20*, 1470–1481.

Robinson, D.G., Scheuring, D., Naramoto, S., and Friml, J. (2011). ARF1 localizes to the golgi and the trans-golgi network. Plant Cell *23*, 846–849; author reply 849-850.

Rodriguez-Furlán, C., Salinas-Grenet, H., Sandoval, O., Recabarren, C., Arraño-Salinas, P., Soto-Alvear, S., Orellana, A., and Blanco-Herrera, F. (2016). The Root Hair Specific SYP123 Regulates the Localization of Cell Wall Components and Contributes to Rizhobacterial Priming of Induced Systemic Resistance. Front Plant Sci *7*, 1081.

Schindelin, J., Arganda-Carreras, I., Frise, E., Kaynig, V., Longair, M., Pietzsch, T., Preibisch, S., Rueden, C., Saalfeld, S., Schmid, B., et al. (2012). Fiji: an open-source platform for biological-image analysis. Nat. Methods *9*, 676–682.

Šmilauerová, M. (2001). Plant root response to heterogeneity of soil resources: Effects of nutrient patches, AM symbiosis, and species composition. Folia Geobot *36*, 337–351.

Spruance, S.L., Reid, J.E., Grace, M., and Samore, M. (2004). Hazard ratio in clinical trials. Antimicrob. Agents Chemother. *48*, 2787–2792.

Stokes, A., Atger, C., Bengough, A.G., Fourcard, T., and Sidle, R.C. (2009). Desirable plant root traits for protecting natural and engineered slopes against landslides. Plant and Soil *324*, 1–30.

Toukura, Y., Devee, E., and Hongo, A. (2006). Uprooting and shearing resistances in the seedlings of four weedy species. Weed Biology and Management *6*, 35–43.

Waghmare, S., Lileikyte, E., Karnik, R., Goodman, J.K., Blatt, M.R., and Jones, A.M.E. (2018). SNAREs SYP121 and SYP122 Mediate the Secretion of Distinct Cargo Subsets. Plant Physiology *178*, 1679–1688.

Wickham, H. (2016). ggplot2: Elegant Graphics for Data Analysis (Springer).

Yang, J., Bak, G., Burgin, T., Barnes, W.J., Mayes, H.B., Peña, M.J., Urbanowicz, B.R., and Nielsen, E. (2020). Biochemical and Genetic Analysis Identify CSLD3 as a beta-1,4-Glucan Synthase That Functions during Plant Cell Wall Synthesis. Plant Cell *32*, 1749–1767.

## Tables

**Table 1** *Arabidopsis thaliana* mutant lines used in this study.

| ***Mutant type*** | ***Mutant*** | ***AGI code[a]*** | ***Mutant line*** | ***Referenced in*** |
|---|---|---|---|---|
| Root hair shape | *cow1-3* | At4g34580 | SALK_0021245 | Böhme *et al.* (2004) |
| | *csld3-1* | At3g03050 | CS899 | Favery *et al.* (2001) |
| | *lrx1-4* | At1g12040 | SALK_057038 | Kim *et al.* (2006) |
| | *rol1-2* | At1g78570 | CS16373 | Diet *et al.* (2006) |
| | *gdi1-2* | At3g07880 | SALK_035400 | Kang *et al.* (2017) |
| Vesicle trafficking | *chc1-2* | At3g11130 | SALK_103252 | Kitakura *et al.* (2011) |
| | *chc2-3* | At3g08530 | SALK_151638 | Bourdais *et al.* (2016) |
| | *syp121* | At3g11820 | - | Assaad *et al.* (2004) |
| | *syp122-1* | At3g52400 | SALK_008617 | Assaad *et al.* (2004) |
| Root exudate composition | *jin1-9* | At1g32640 | SALK_017005 | Anderson *et al.* (2004) |
| | *pdr2* | At4g15230 | SAIL_811_F08 | Badri *et al.* (2008) |
| | *pft1-3* | At1g25540 | SALK_059316 | Kidd *et al.* (2009) |
| Unknown | *abcg43-1* | At4g15236 | N75206[b] | This study |
| | *abcg43-2* | At4g15236 | SALK_201207 | This study |
| | *abcg43-3* | At4g15236 | SALKseq_30713 | This study |

## Figure legends

**Fig. 1** Physical root hair properties contribute to root-substrate adhesion in *Arabidopsis thaliana*.

(a) Root hair phenotypes of 5-d-old wild-type (Col-0), *lrx 1-4, csld3-1, cow1-3, rol1-2,* and *gdi1-2* seedlings grown on gel medium and statistical comparisons of mean root hair density (number per mm length of root) and mean root hair length (mm) for each mutant line relative to wild type. White asterisks on the root hair images indicate the characteristic root hair bulging phenotype in the *lrx1-4* mutant and the short, branching root hair phenotype in *gdi1-2*. Scale bar = 0.25 mm. In the table, the mean ± standard error is given for root hair density and root hair length of wild type and each mutant as well as a mean comparison to wild type, which is listed in bold. "No difference" is stated when there was no statistically significant difference between wild type and a mutant line. The statistical output of each univariate linear model is given. Alpha = 0.025, statistical significance codes: '***' = < 0.001, '**' = < 0.01. The results shown are from a representative experiment for at least two independent experiments. Survival curves displaying the proportion of seedlings that adhered to the gel at increasing centrifugal force for (b) 92 wild type (Col-0 – black); 81 *lrx1-4* (light green); 70 *csld3-1* (green); (c) 82 wild type (Col-0 - black); 83 *cow1-3* (green); and (d) 77 wild type (Col-0- black); 85 *rol1-2* (light green); and 86 *gdi1-2* (dark green). Circled red crosses on the survival curves represent seedlings that remained adhered to the gel after the maximum centrifugal speed (1611 RPM). The results shown are from a representative experiment for at least two independent experiments showing a statistically significant difference in adhesion between mutant lines relative to wild type (Cox PH regression; alpha = 0.01). A single experiment included ≥ 70 biological replicates for each candidate line.

**Fig. 2** Vesicle trafficking mechanisms that contribute to root-substrate adhesion in *Arabidopsis thaliana*.

(a) Root hair phenotypes of 5-d-old wild-type (Col-0), *syp121, syp122-1, chc1-2* and *chc2-3* seedlings grown on a gel medium and statistical comparisons of mean root hair density (number per mm length of root) and mean root hair length (mm) for each mutant line relative to wild type. Scale bar = 0.25 mm. In the table, the mean ± standard error is given for the root hair density and root hair length of wild type and each mutant as well as a mean comparison to wild type, which is listed in bold. "No difference" is stated when there was no statistically significant difference between wild type and a mutant line. The statistical output of each univariate linear model is given. Alpha = 0.025. The results shown are from a representative experiment for at least two independent experiments. Survival curves displaying the

proportion of seedlings that adhered to the gel at increasing centrifugal force for (b) 87 wild type (Col-0 – black); 91 *syp121* (turquoise); 83 *syp122-1* (blue/grey); and (c) 83 wild type (Col-0 – black); 70 *chc1-2* (dark blue)*;* and 72 *chc2-3* (medium blue). Red crosses circled on the survival curves represent seedlings that remained adhered to the gel after the maximum centrifugal speed (1611 RPM). The results shown are from a representative experiment for at least two independent experiments showing a statistically significant difference in adhesion between all mutant lines relative to wild type (Cox PH regression; alpha = 0.01). A single experiment included $\geq$ 70 biological replicates for each candidate line.

**Fig. 3** Exudate composition changes root-substrate adhesion properties in *Arabidopsis thaliana*.

(a) Root hair phenotypes of 5-d-old wild-type (Col-0), *jin1-9*, *pdr2* and *pft1-3* seedlings grown on a gel medium and statistical comparisons of mean root hair density (number per mm length of root) and mean root hair length (mm) for each mutant line relative to wild type. Scale bar = 0.25 mm. In the table, the mean ± standard error is given for the root hair density and root hair length of wild type and each mutant as well as a mean comparison to wild type, which is listed in bold. "No difference" is stated when there was no statistically significant difference between wild type and a mutant line. The statistical output of each univariate linear model is given. Alpha = 0.025. The results shown are from a representative experiment for at least two independent experiments. (b) Survival curves displaying the proportion of seedlings that adhered to the gel at increasing centrifugal force for 80 wild type (Col-0 – black), 81 *jin1-9* (light pink), 80 *pdr2* (light orange), and 81 *pft1-3* (dark orange). The results shown are from a representative experiment for at least two independent experiments showing a statistically significant difference in adhesion between mutant lines relative to wild type (Cox PH regression; alpha = 0.01), except for *jin1-9*. A single experiment included $\geq$ 70 biological replicates for each candidate line.

**Fig. 4** Using the centrifuge assay in a forward genetic screen to identify *Arabidopsis thaliana* root-substrate adhesion mutants.

(a) T-DNA insert locations in *ABCG43* for each *abcg43* mutant allele, with insertions indicated by orange arrowheads. The *ABCG43* gene is located on chromosome four at position Chr4: 8,969,677-8,702,727 and contains 23 exons (dark green) and 22 introns (white gaps). *abcg43-1* has a T-DNA insert in the exon10/intron10 boundary, *abcg43-2* (SALK_201207) has a T-DNA insert in exon 2 and *abcg43-3* (SALKseq_30713) has a T-

DNA insert in exon 3. (b) Genomic PCR confirming the homozygosity of each *abcg43* mutant for the respective T-DNA inserts. Lanes **1** and **2** were loaded with the gene-specific and T-DNA-border PCR products from *abcg43* mutant lines. Lanes **3** and **4** were loaded with the gene-specific and T-DNA-border PCR products from a wild type (Col-0) genomic DNA template. Lanes **5** and **6** were loaded with the water controls for the gene-specific and T-DNA-border PCR reactions, respectively. '**L'** indicates the 100-bp ladder. The expected product sizes for the gene-specific PCRs were ~350 nt, ~1025 nt and ~1090 nt; the T-DNA-border PCR product sizes were ~400 nt, ~550 nt and ~750 nt for *abcg43-1*, *abcg43-2* and *abcg43-3* alleles, respectively. (c) Survival curves displaying the proportion of seedlings that adhered to the gel at increasing centrifugal force for 79 wild type (Col-0 – black), 70 *abcg43-1* (dark pink), 85 *abcg43-2* (purple), and 73 *abcg43-3* (light purple). Red crosses circled on the survival curves represent seedlings that remained adhered to the gel after the maximum centrifugal speed (1611 RPM). The results are from a representative experiment for at least two independent experiments showing a statistically significant difference in adhesion between the mutant lines relative to wild type (Cox PH regression; alpha = 0.01). A single experiment included $\geq$ 70 biological replicates for each candidate line.

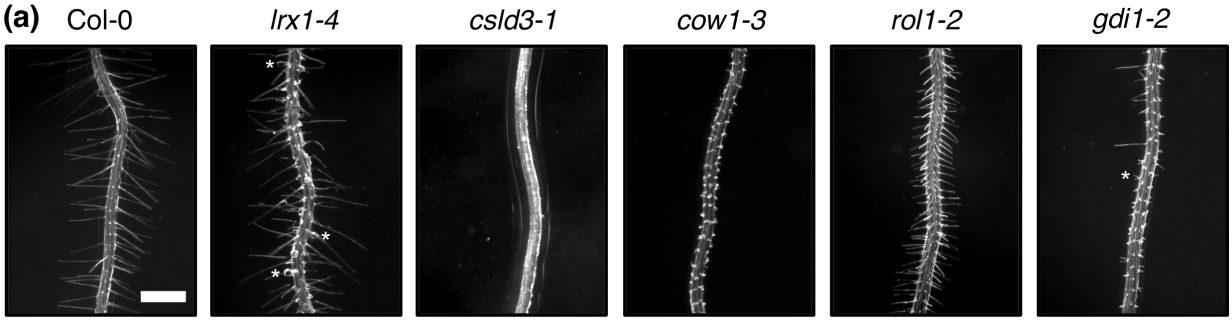


| Line | Root hair density (number per mm length of root) | | Root hair length (mm) | |
|---|---|---|---|---|
| Col-0 | 30.556 ± 0.784 | - | 0.518 ± 0.009 | - |
| *lrx1-4* | 31.889 ± 0.935<br>**No difference** | t = 1.093, P > 0.05<br>d.f. = 16, *n* = 9 | 0.388 ± 0.008<br>**1.3 times shorter**** | t = -2.819, P < 0.001<br>d.f. = 16, *n* = 9 |
| *csld3-1* | 8.778 ± 1.188<br>**3.5 times less***** | t = -15.30, P < 0.001<br>d.f. = 16, *n* = 9 | 0.045 ± 0.002<br>**10.1 times shorter***** | t = -11.790, P < 0.001<br>d.f. = 16, *n* = 9 |
| *cow1-3* | 29.200 ± 0.772<br>**No difference** | t = -1.23, P > 0.05<br>d.f. = 17, *n* = 10 | 0.049 ± 0.001<br>**10 times shorter***** | t = -12.37, P < 0.001<br>d.f. = 17, *n* = 10 |
| *rol1-2* | 30.700 ± 1.550<br>**No difference** | t = 0.08, P > 0.05<br>d.f. = 17, *n* = 9 | 0.195 ± 0.003<br>**2.7 times shorter***** | t = -8.417, P < 0.001<br>d.f. = 17, *n* = 10 |
| *gdi1-2* | 26.200 ± 1.041<br>**0.17 times less**** | t = -3.282, P < 0.01<br>d.f. = 17, *n* = 9 | 0.135 ± 0.006<br>**3.8 times shorter***** | t = -9.04, P < 0.001<br>d.f. = 16, *n* = 9 |

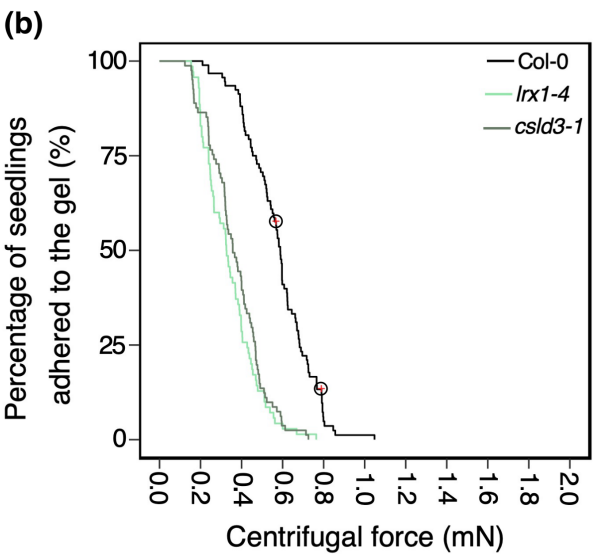


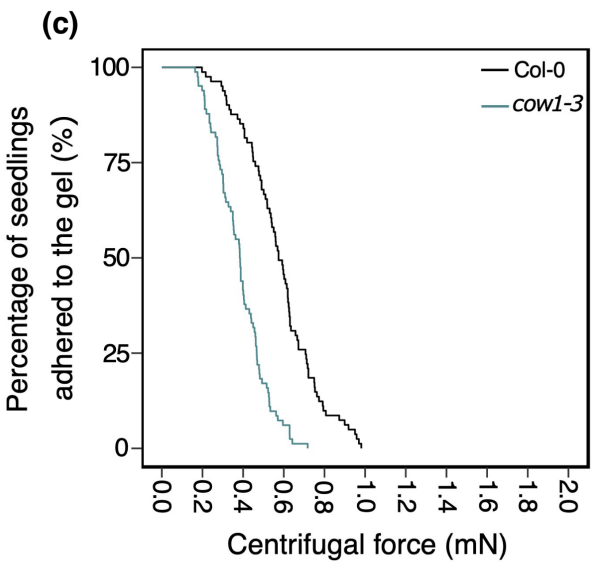


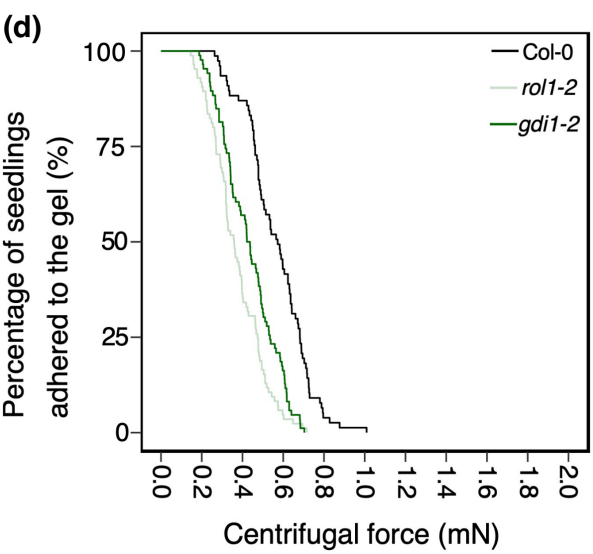

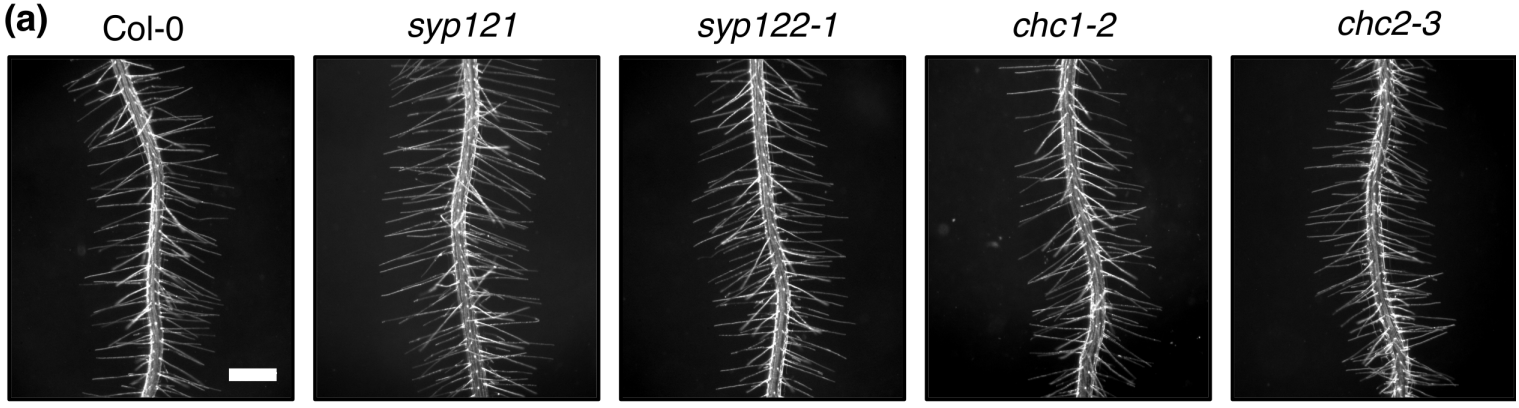


| Line | Root hair density (number per mm length of root) | | Root hair length (mm) | |
|---|---|---|---|---|
| Col-0 | 32.000 ± 0.632 | - | 0.420 ± 0.005 | - |
| *syp121* | 31.200 ± 0.952<br>**No difference** | t = -0.700, P > 0.05<br>d.f. = 18, *n* = 10 | 0.461 ± 0.004<br>**No difference** | t = 1.974, P > 0.05<br>d.f. = 18, *n* = 10 |
| *syp122-1* | 32.200 ± 0.442<br>**No difference** | t = 0.259, P > 0.05<br>d.f. = 18, *n* = 10 | 0.452 ± 0.005<br>**No difference** | t = 1.379, P > 0.05<br>d.f. = 18, *n* = 10 |
| *chc1-2* | 30.889 ± 0.716<br>**No difference** | t = -1.168, P > 0.05<br>d.f. = 17, *n* =9 | 0.441 ± 0.006<br>**No difference** | t = 0.684, P > 0.05<br>d.f. = 17, *n* = 9 |
| *chc2-3* | 31.889 ± 0.790<br>**No difference** | t = -0.111, P > 0.05<br>d.f. = 17, *n* = 9 | 0.463 ± 0.006<br>**No difference** | t = 0.182, P > 0.05<br>d.f. = 18, *n* = 10 |

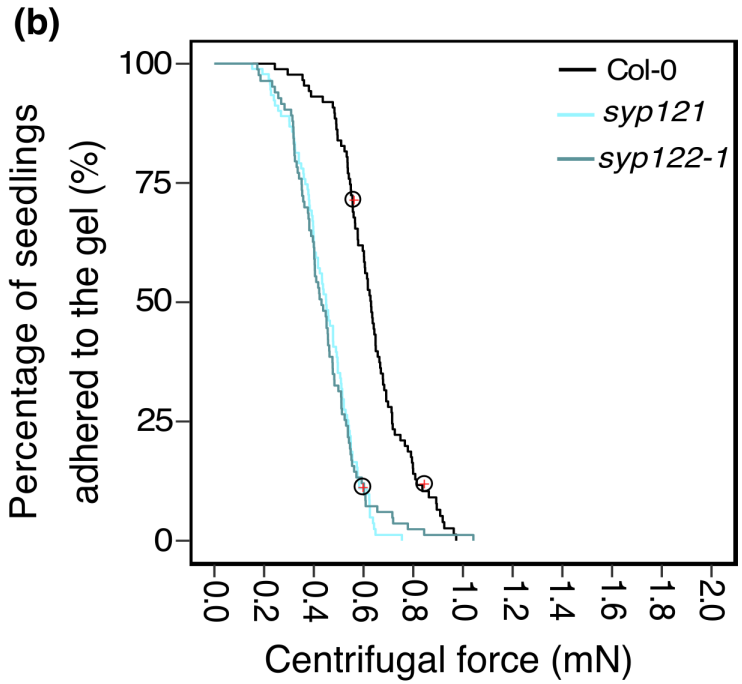


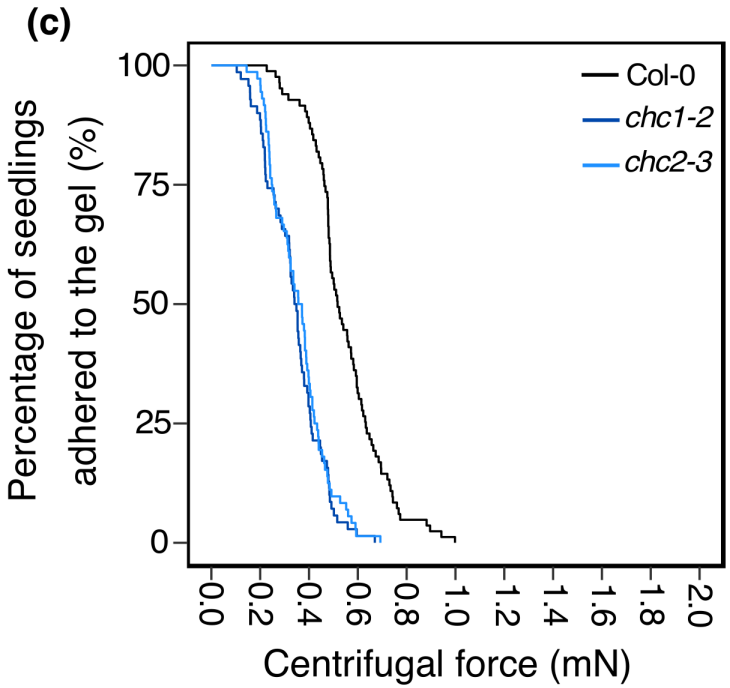

(a)

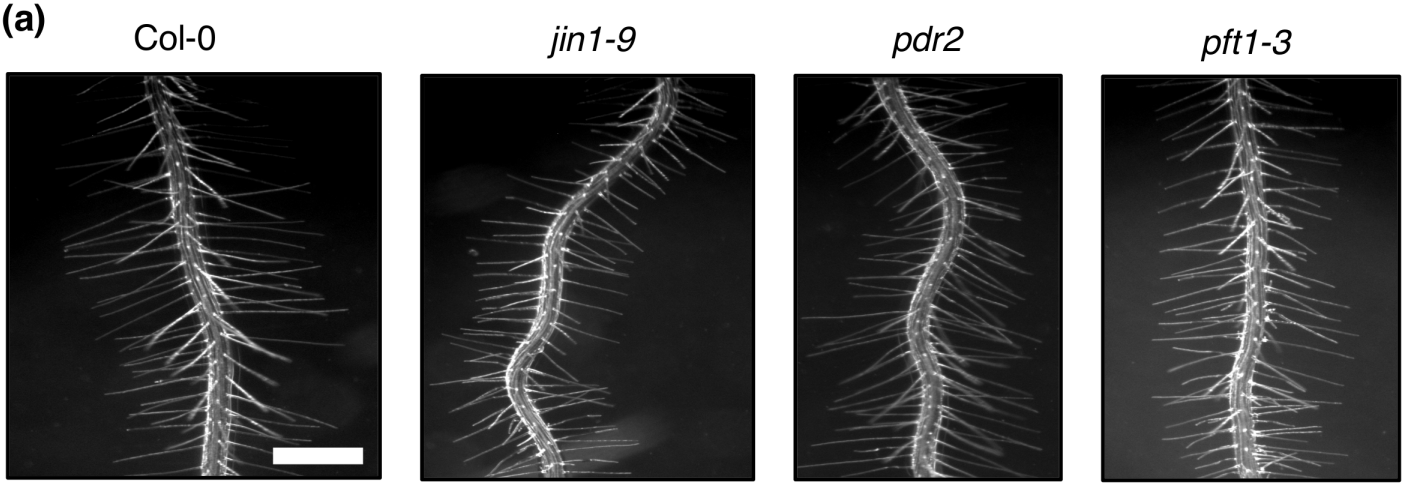


| Line | Root hair density (number per mm length of root) | | Root hair length (mm) | |
|---|---|---|---|---|
| Col-0 | 30.111 ± 1.612 | - | 0.416 ± 0.005 | - |
| *jin1-9* | 29.444 ± 1.271<br>**No difference** | t = -0.324, P > 0.05<br>d.f. = 16, *n* = 9 | 0.429 ± 0.006<br>**No difference** | t = 0.555, P > 0.05<br>d.f. = 16, *n* = 9 |
| *pdr2* | 31.125 ± 0.854<br>**No difference** | t = 0.533, P > 0.05<br>d.f. = 15, *n* =8 | 0.428 ± 0.006<br>**No difference** | t = 0.521, P > 0.05<br>d.f. = 15, *n* = 8 |
| *pft1-3* | 29.000 ± 1.179<br>**No difference** | t = -0.555, P > 0.05<br>d.f. = 16, *n* = 9 | 0.424 ± 0.006<br>**No difference** | t = 0.295, P > 0.05<br>d.f. = 16, *n* = 9 |

(b)

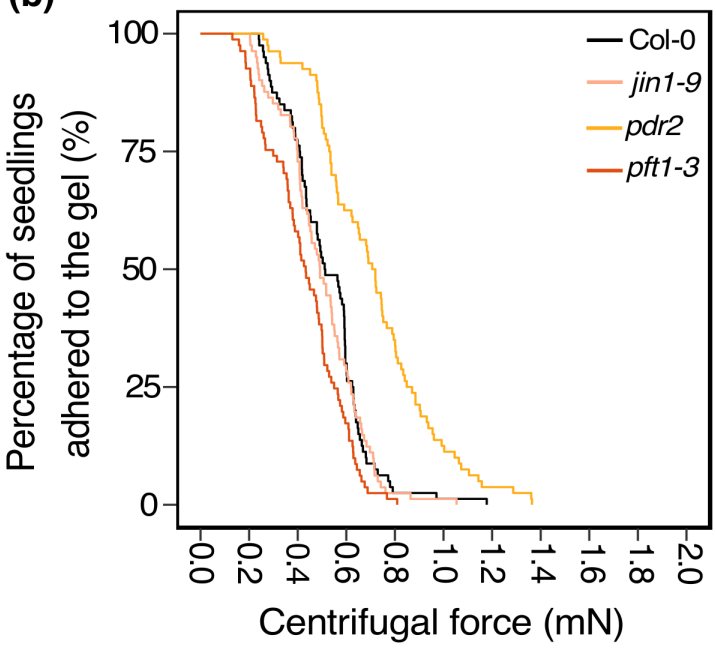

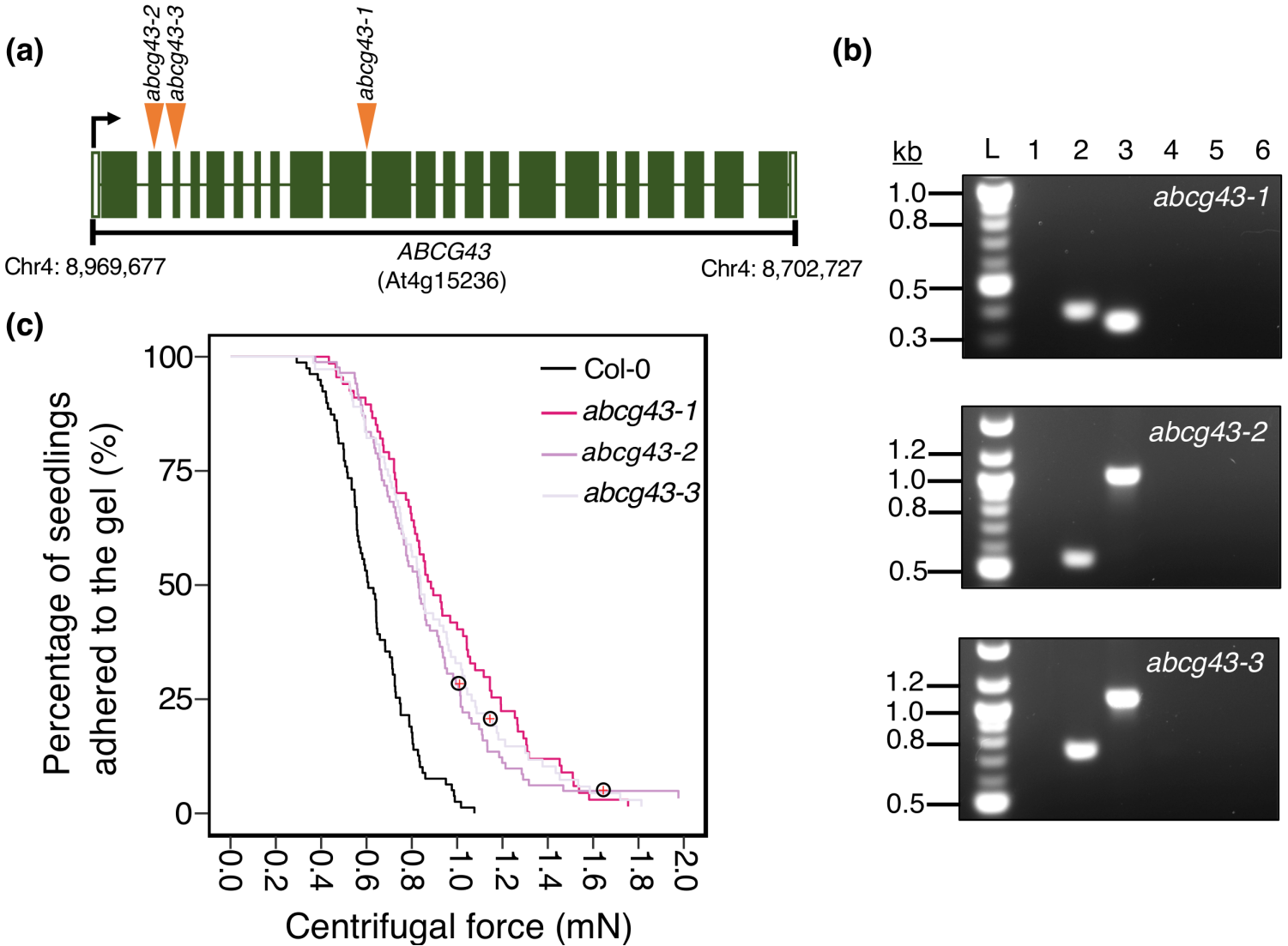
(a)
abcg43-2
abcg43-3
abcg43-1
Chr4: 8,969,677
ABCG43
(At4g15236)
Chr4: 8,702,727
(b)
kb
L 1 2 3 4 5 6
1.0
0.8
0.5
0.3
abcg43-1
1.2
1.0
0.8
0.5
abcg43-2
1.2
1.0
0.8
0.5
abcg43-3
(c)
Percentage of seedlings adhered to the gel (%)
100
75
50
25
0
Col-0
abcg43-1
abcg43-2
abcg43-3
0.0 0.2 0.4 0.6 0.8 1.0 1.2 1.4 1.6 1.8 2.0
Centrifugal force (mN)